Aquaculture 563 (2023) 738990

Contents lists available at ScienceDirect

Aquaculture

journal homepage: www.elsevier.com/locate/aquaculture

Comparative analysis of genetic diversity and structure among four shell color strains of the Pacific oyster *Crassostrea gigas* based on the mitochondrial COI gene and microsatellites

Yifei Zhang [a], Yulu Chen [a], Chengxun Xu [a], Qi Li [a,b,*]

[a] Key Laboratory of Mariculture, Ministry of Education, Ocean University of China, Qingdao 266003, China
[b] Laboratory for Marine Fisheries Science and Food Production Processes, Qingdao National Laboratory for Marine Science and Technology, Qingdao 266237, China

ARTICLE INFO

Keywords:
Crassostrea gigas
Shell color quantification
Genetic diversity
Microsatellite
Artificial selection

ABSTRACT

Shell color is one of the major determinants in the popularity of shelled seafood. To enhance the commercial value of the Pacific oyster (*Crassostrea gigas*), four shell color strains of black (SB), white (SW), gold (SG), and orange (SO) were bred purposefully for 11–12 generations. In this study, CIELAB colorimetric analysis was used to evaluate the effectiveness of shell color selection of *C. gigas*. The color parameters (L^*, a^*, b^*) by statistical analysis differed significantly across black, white, gold, and orange shell strains ($P < 0.05$), and the principal component analysis characterized the considerable improvement in shell color uniformity. Further, we carried out genetic analysis by 15 microsatellites and mitochondrial cytochrome oxidase I sequences (mtCOI). A total of 121 alleles were detected at all 15 microsatellite loci, with the average number of alleles per locus ranging from 4.07 in SO to 7.67 in SW. Compared with wild populations, the shell color strains had significantly fewer alleles and mtCOI haplotypes, but the average heterozygosity, including H_o from 0.52 to 0.66 and H_e from 0.59 to 0.75, was not statistically different ($P < 0.05$). The SO samples suffered the greatest loss of diversity and occupied the lowest value of all genetic diversity indices, which is likely due to the smaller size of founding stock resulting in a stronger bottleneck. Population simulation analysis showed that the genetic background of four shell color strains was completely separated, confirming the consistency of phenotypically defined and genetically differentiated populations. Pairwise F_{ST} calculated by microsatellites with a range of 0.267 to 0.121 revealed high levels of genetic differentiation among strains, which has far exceeded the divergence between different geographical populations of *C. gigas* (F_{ST}: 0.012–0.034). The results obtained in the study provide valuable information for further genetic improvement of shell color variants through selective breeding.

1. Introduction

Mollusca is generally considered to be the largest phylum in the marine realm, and the majority of them, including nearly all bivalves and most gastropods, are covered with shells (Williams, 2017). As shelled mollusks grow, various types of pigments are secreted by mantle along the growing edge and then incorporated into different layers of shell, usually the outermost, eventually resulting in highly varying colors and patterns on surface (Budd et al., 2014). Such phenotypic differences, just like unique tags, are more suitable as genetic markers for population categorization and identification than other morphological features (Tettelbach et al., 2020). More importantly, surface color is an important marketing characteristic for shelled marine products due to its significant impact on consumers' visual perception and preference for choice (Kahn and Wansink, 2004). Rich color morphs can provide substantial numbers of variants for selective breeding, which breathes new life into the seafood market ceaselessly.

In nature, intraspecific color polymorphism tends to be more common in bivalves such as the Triangle pearl mussel *Hyriopsis cumingii* (Wen et al., 2013), the Manila clam *Ruditapes philippinarum* (Nie et al., 2020), and the Pacific oyster *Crassostrea gigas* (Song et al., 2017), all of which are composed of two or more distinct color phenotypes. The availability of multiple shell color variants from wild stocks makes it feasible to understand the genetic basis of color determination, which is the precondition to start efficient genetic improvement of shell color traits. There is accumulating evidence suggesting that shell

* Corresponding author at: Key Laboratory of Mariculture, Ministry of Education, Ocean University of China, Qingdao 266003, China.
E-mail address: qili66@ouc.edu.cn (Q. Li).

https://doi.org/10.1016/j.aquaculture.2022.738990
Received 27 August 2022; Received in revised form 20 October 2022; Accepted 21 October 2022
Available online 28 October 2022

pigmentation is highly heritable and controlled by a limited number of genes with straightforward patterns of dominance (Brake et al., 2004; Zheng et al., 2013). Abiotic factors, including diet (Marchais et al., 2017), temperature (Phifer-Rixey et al., 2008), and salinity (Sokolova and Berger, 2000), also induce the variation of chromaticity and brightness, but such modifications caused by the environment are not determinants of color polymorphism. Thus, theoretically speaking, appropriate test-mating can separate the exact genotype of shell color trait followed by consecutive directional selection to fix the major genes, and then the selective target can be accomplished within several generations (Evans et al., 2009). In practice, the genetic improvement of shell color has been carried out in many economically important aquatic species, and multiple new color varieties have been developed successfully through selective breeding programs. For example, a genetically stable white-shell line of the Japanese pearl oyster *Pinctada fucata martensii*, infrequent in natural populations, was obtained over five generations of selection (Wada, 1990). Similarly, different-colored shell stocks of orange, purple, and white were established by selective breeding in the bay scallop *Argopecten irradians irradians* (Zheng et al., 2005). In addition, diverse shell color variants of the north-Chilean scallop *Argopecten purpuratus* were also bred successfully (Winkler et al., 2001).

There is no denying that the sustainability of selective breeding programs is a prerequisite for the cultivation of new varieties. The level of genetic diversity, i.e., the richness of genetic information determines the biological survivability and environmental adaptation and is, therefore, a basis for the long-term preservation of breeds (Boudry et al., 2002). Furthermore, sufficient genetic diversity is also required for sustained genetic improvement and stable inheritance of desirable traits (Evans et al., 2004a). Usually, no new genetic resources are introduced into breeding populations, which may reduce the genetic diversity of these artificially closed populations through selective pressure and inbreeding repression (Chen et al., 2017). However, the degree of such an impact varies greatly across populations and species, so it is necessary to analyze the changing trend of genetic diversity on a case-by-case basis. Similar to wild populations, aquaculture stocks, especially those propagated for specific characteristics, are subject to various biological and anthropogenic factors that aggregate into the evolutionary forces shaping genetic structure (Berrebi et al., 2021). Investigating the extent of genetic divergence among cultured populations, not only to trace the stock origin and mixing but also to gain insights into breeding practices and the domestication process, is another important aspect of hatchery management.

The Pacific oyster (*Crassostrea gigas*) is an aquaculture species of considerable economic importance on a global scale, and effective genetic improvement around this species can boost its commercial value continuously (Dégremont et al., 2010; Li et al., 2011). As the demand for live and half-shell oysters continues to increase, the shell appearance becomes the consumer's first impression of oyster quality. Proof by facts, a rare bronze-shell variant of *C. gigas* was more appealing than the common ones in shelled seafood market (Nell, 2001). Likewise, oysters with uniformly dark shell fetched a much higher price in Korea (Kang et al., 2013). In this context, the manipulation of shell color trait of *C. gigas* through selective breeding programs as a method of improving oyster quality is timely and promising in terms of marketing. In our previous breeding process, the precious and purified shell color strains of black, white, gold, and orange were developed. In this study, CIELAB colorimetric analysis was used to digitally capture the phenotypic characteristics to impartially assess the efficacy of shell color selection in *C. gigas*, and then a comprehensive picture of population genetic differentiation and levels of diversity was evaluated based on the combination of 15 microsatellites and mitochondrial COI sequences. Further, we compared genetic information of shell color strains with that of four wild populations of *C. gigas* previously published by Chen et al. (2022) to examine the driving role of artificial selection.

2. Materials and methods

2.1. Sample collection and DNA extraction

Four selected strains used in this study were the black shell strain (SB), white shell strain (SW), gold shell strain (SG), and orange shell strain (SO) of the Pacific oyster. In 2010, the base populations of SB, SW, and SG were collected from wild oysters with specific shell colors in coastal areas of Shandong Province, China, and one hundred broodstocks (50 sires and 50 dams) were used to establish 50 full-sib families as the first generation. While the orange shell strain was established using only four rare variants (two males and two females) with orange left and right shells that were discovered in the progeny of purple-black shell color oysters, then these four individuals were used as parents to produce two full-sib families as the first generation in 2011. Subsequently, the family selection was constructed across three consecutive generations in the strains of SB, SW, and SG from 2011 to 2013, and across two generations in SO from 2012 to 2013 to accumulate pigmentation. The criteria of broodstock choosing in family-based selection were individuals with deeper pigmentation degree and/or greater pigment coverage from families with higher shell color purification rates and without color separation. Next, mass selections were initiated in 2014 to enhance the growth performance of shell color strains. Briefly, size-frequency distribution was determined for stocks using standard shell height before selection, and the broodstocks were selected from the top end of the size distribution, but only included oysters fully covered with desirable color. In each generation, approximately 75 to 100 parents in all were selected according to the above criteria for dissection to obtain sperm and eggs, and artificial fertilization was performed after estimating oocyte concentration by the microscope to provide equal mating chances for each female and male. After fertilization, embryos were incubated for about 22 h in hatching tanks, in which fertilized eggs developed into D-larvae. The rearing from larvae metamorphosing to spats was carried out according to standard procedures by Li et al. (2011) while maintaining consistent living conditions for all four shell color variants. Then the spats were deployed to the coastal area of Rongcheng in the Yellow Sea, China, where they were strung up on nylon ropes and cultured on suspended longlines.

By 2021, the SB, SW, and SG strains have gone through twelve generations of selective breeding, while the SO strain has been selected for the eleventh generation. The number of broodstock and sex ratio are shown in Table 1. We collected 48 samples from each color strain randomly in November 2021 (Fig. 1), and all of them grew up in the cultured area in Rongcheng. Besides, four wild populations distributed in Rongcheng (RC, 37.1°N, 122.5°E), Qingdao (QD, 36.1°N, 120.3°E), Lianyungang (LYG, 34.9°N, 119.3°E), and Zhoushan (ZS, 30.1°N, 121.1°E) were collected. The adductor muscle of each oyster was separated and immediately conserved in absolute ethyl alcohol at -30 °C. The purity and concentration of genomic DNA were determined using a NanoDrop 2000 after extraction using the standard procedure of the phenol-chloroform method (Li et al., 2006). Samples for mtDNA analysis were selected from the same individuals used for nuclear DNA analysis.

2.2. Shell color measuring and statistical analysis

The computer vision system (CVS) captures pictures with a digital camera and then utilizes image analysis software to extract color parameters, allowing for a precise and impartial assessment of color patterns on uneven surfaces (Pedreschi et al., 2006). The CIELAB color space, which describes all colors visible to the human eye, is the international color measuring standard specified by the Commission International d' Eclairage (CIE) (Timmermans, 1998). L^* represents the lightness component from 0 (completely black) to 100 (completely white); parameters a^* (from green to red) and b^* (from blue to yellow) are two color quality indexes, which range from −120 to 120; ΔE

Table 1
List of sample information and the effective population size (N_b) in shell color strains and wild populations of *C. gigas*.

Population	Number of parents		Sample time	Sample size		Effective population size (N_b)	
	Female	Male		Microsatellite	mtCOI	N_b	95% CI (lower-upper)
SB	50	50	11/2021	48	20	86.7	63.8–158.6
SW	50	50	11/2021	48	20	79.9	59.7–142.7
SG	50	50	11/2021	48	20	73.5	82.6–135.9
SO	50	50	11/2021	48	20	66.4	50.5–102.1
RC	–	–	12/2020	48	20	498.6	367.3–637.3
QD	–	–	12/2020	48	20	198.3	147.3–296.7
LYG	–	–	12/2020	48	20	595.3	344.3–605.3
ZS	–	–	12/2020	48	20	479.0	209.7–499.2

Fig. 1. Four Pacific oyster strains with black (SB), white (SW), gold (SG), and orange (SO) shells in the study. (For interpretation of the references to color in this figure legend, the reader is referred to the web version of this article.)

represents the color difference between every sample and the typical one. Oyster shells were cleaned with caution and dried in the shade before being measured. All of the left shells were photographed with a digital camera (Nikon D80) under the standard capture conditions (Evans et al., 2009). The raw color components, including lightness, a and b values, were extracted from the digitalized images using Photoshop CS6 (Adobe System Incorporated, USA) and then transformed into standard $L^*a^*b^*$ values referring to the following formulas (Yam and Papadakis, 2004):

$$L^* = \frac{Lightness}{255} \times 100$$

$$a^* = \frac{240a}{255} - 120$$

$$b^* = \frac{240b}{255} - 120$$

$$\Delta E = \sqrt{(L^* - L^*) + (a^* - a^*) + (b^* - b^*)}$$

A preliminary statistical analysis of the parameters $L^*a^*b^*$ describing shell color was completed using IBMSPSS Statistics 20.0 (IBM, USA). Then, the two principal components with the top cumulative contribution were extracted from color variables by principal component analysis (PCA), and the results were further visualized using OriginPro 2022b software (OriginLab, USA) to show differences in shell color among strains.

2.3. Microsatellite analysis

Overall, the genomic DNA of 192 oysters from four shell color strains was amplified using 15 microsatellite primers, originally designed from the Pacific oyster and widely used in previous studies (Li et al., 2003; Sekino et al., 2003; Yamtich et al., 2005; Qi et al., 2009; Sauvage et al., 2009). Following the principle of efficiency and economy, all selected microsatellite loci were divided into six multiplex PCR sets, including Panel 1 (ucdCg-117, ucdCg-120, and ucdCg-198), Panel 2 (Crgi3, ucdCg-146, and uscCgi-210), Panel 4 (otgfa0_0129_E11 and otgfa0_0007_B07), Panel 5 (ucdCg-152 and Crgi39), Panel 6 (ucdCg200 and otgfa0_408293) developed by Liu et al. (2017), and one additional panel (ucdCg-140, ucdCg-112, and Cgsili57) developed by Chen et al. (2022). The final volume of multiplex PCRs was 10 μL containing 50 ng template DNA, 0.25 U 2× PCR Master Mix, 0.15 μmol/L forward primer, 0.06 μmol/L reverse primer, and 0.15 μmol/L universal tailed primer M13 (−21) with different fluorescent dyes (NED, HEX, and VIC). The amplification conditions comprised an initial denaturing period of 95 °C for 3 min followed by 35 cycles of 15 s denaturing at 95 °C, 40 s at the optimal annealing temperature, and 60 s at 72 °C; then 8 cycles of 15 s at 93 °C, 20 s at 53 °C, 60 s at 72 °C and a final 10-min extension step at 72 °C. After checking the amplified products on agarose gel, genotyping was performed on ABI PRISM 3130 Automated DNA Sequencer (Applied Biosystems) using the internal standard GeneScan LIZ 500. Raw allelic data over 15 loci from four wild populations (Chen et al., 2022) were added to the subsequent data analysis.

The size of alleles was defined automatically by GeneMarker v.2.2.0 (Applied Biosystems) and then verified manually one by one. MicroChecker v.2.2.3 (Van Oosterhout et al., 2004) was used to correct stuttering or large allele dropouts that occurred during the interpretation of sequences of microsatellite allele data. The Fisher's exact test was implemented in Genepop v.4.0 (Rousset, 1995) to detect deviations from Hardy-Weinberg equilibrium (*HWE*). Basic parameters of genetic diversity, including the number of alleles (*N*), number of effective alleles (N_e), inbreeding coefficient (F_{is}), Shannon-Wiener index (*I*), observed (H_o) and expected heterozygosity (H_e), were calculated using GenAlEX v.6.5 (Peakall and Smouse, 2012), and the polymorphism information content (*PIC*) was performed by CERVUS v.3.0 (Kalinowski et al., 2007). A nonparametric analysis of variance (Kruskal-Wallis test) was used to address the differences in the above statistical parameters. The frequencies of null alleles for each locus and population were tested by

FreeNA software (Chapuis and Estoup, 2007). The INA (including null alleles) correction method was then performed according to Chapuis et al. (2008), simply by systematically changing the estimated false homozygous genotypes XX induced by the null allele to X999 to reduce the bias in genetic diversity. The adjusted data set was used to recalculate H_o, H_e, F_{is}, and the number of loci deviating from *HWE* using the methods described above.

The individual-based assignment test was conducted in STRUCTURE v.2.3 (Falush et al., 2003) to determine the optimal number of genetic clusters (K). We utilized the admixture ancestry model under the correlated allele frequency model. For the parameter settings, twenty independent runs were undertaken with a simulation of 5000 length Burn-in phase for each of the assumed K values (ranging from 2 to 10), and the number of Markov chain Monte Carlo (MCMC) repetitions was set at 50,000 after Burn-in for each run. Then the Delta K graph from structure analysis was obtained by Structure Harvester software (Evanno et al., 2005). The proportional membership of each genetic cluster was estimated for each individual and population. Further, population genetic variance was analyzed by the analysis of molecular variance (AMOVA) performed on ARLEQUIN v.3.5 (Excoffier and Lischer, 2010) using genotype data set corrected by the INA method. Given that the presence of null alleles is known to lead to an overestimation of both F_{ST} and genetic distance, the Weir's unbiased estimator of F_{ST} and the genetic distance of Cavalli-Sforza and Edwards (D_C) were calculated by the ENA correction method (excluding null alleles) in FreeNA software (Chapuis and Estoup, 2007). In contrast to INA, the ENA method, independent of the level of gene flow and the number of loci, nearly entirely eliminated the bias in genetic differentiation caused by null alleles (Chapuis and Estoup, 2007). To visualize the genetic distance among the samples in the orthogonal space directly, the principal coordinates analysis (PCoA) was performed on GenAlEX v.6.5. All the samples with similar compositions would appear in close proximity to each other and can be easily clustered together.

In addition, effective population sizes based on the linkage disequilibrium method (N_b) were identified by NeEstimator v.2.1 (Do et al., 2014). The N_b estimates produced did not include alleles with frequencies <0.05, and 95% confidence intervals (95% CI) were also reported.

2.4. Mitochondrial COI analysis

Twenty samples were randomly selected from each shell color strain to amplify the mitochondrial cytochrome C oxidase subunit I (mtCOI) sequences using universal primers LCO1490 and HCO2198 (Vrijenhoek, 1994). PCR products were purified and sequenced from the forward direction by the Personal Company (Shanghai, China). The sequences obtained required further processing, including the use of SeqMan to eliminate ambiguous bases and MEGA to modify and align. The indexes of molecular diversity such as haplotype diversity (H_d), percent nucleotide diversity (P_i), and average number of nucleotide differences (k) were calculated by DNASP v.5.10 (Librado and Rozas, 2009). The distribution and evolutionary relationships for the mtDNA haplotypes were displayed in the Median-joining (MJ) networks (Bandelt et al., 1999) constructed by Popart 1.7 (Leigh and Bryant, 2015). The estimations of F_{ST} and the analysis of AMOVA were performed on ARLEQUIN v.3.5. Also, the mtCOI sequences of wild populations derived from a random sample of 80 individuals were analyzed according to the same procedure.

3. Results

3.1. Quantitative analysis of shell color

The descriptive statistics for the color parameters in the SB, SW, SG and SO are listed in Table 2. Differential analysis indicated significant variations ($P < 0.05$) between strains in each shell color value (including L^*, a^*, and b^*). The range of L^* varied from 20.46 to 69.70, with the maximum and minimum values seen in the SW and SB, respectively. The lowest values of a^* and b^* were both in the SW, whereas the highest values of a^* and b^* were 12.19 in the SO and 36.67 in the SG, separately. In addition, the L^* values of all strains had a wider fluctuation range, indicating that the genetic stability of parameter L^* was inferior to that of a^* and b^* in general (Wan et al., 2017; Xu et al., 2017). Two main principal components, PC1 and PC2, were extracted from three color parameters through principal component analysis (PCA), and their cumulative contribution rates to the overall variances reached up to 87.70%. The first principal component (PC1), accounting for 51.70% of the total variances, was affected mainly by a^* (0.730) which can be regarded as the primary factor causing the difference in shell color (Table 2).

Table 2
Descriptive statistics of the color parameters in the black, white, gold and orange strains of *C. gigas* and factor loadings of principal components extracted from three shell color parameters.

Color parameter	SB	SW	SG	SO	PC1	PC2
L^*	20.46 ± 4.39^a	69.70 ± 4.20^b	54.26 ± 5.76^c	34.36 ± 7.63^d	−0.345	0.830
a^*	3.40 ± 0.99^a	1.32 ± 0.73^b	6.24 ± 2.17^c	12.19 ± 2.13^d	0.730	−0.057
b^*	7.34 ± 2.40^a	3.57 ± 1.96^b	36.67 ± 3.55^c	18.61 ± 3.35^d	0.591	0.555
ΔE	6.76 ± 4.33	6.57 ± 3.61	7.58 ± 3.13	10.24 ± 6.02		
Contribution ratio					0.517	0.360

PC: principal component. Means in the same line superscripted by different letters were significantly different ($P < 0.05$).

Fig. 2 depicts the scatter plot of the two principal components, PC1 and PC2. It's obvious that the data points of the four strains had their own distribution areas with almost no overlapping. The distinct separation suggested that the shell color trait of each strain was quite consistent after being selectively bred. In addition, the data points of SO and SG were relatively dispersive, while the more concentrated data points, implying a higher purifying efficiency, appeared in SB and SW.

3.2. Genetic diversity revealed by microsatellites and mtDNA region

In general, 15 microsatellite loci were selected for genotyping 384 oysters from four shell color strains (SB, SW, SG, SO) and four wild populations of *C. gigas* (LYG, QD, RC, ZS). There was no obvious scoring error caused by large allele dropout and/or stuttering at any loci. The estimated frequencies of null alleles per locus were from 0.043 to 0.263, of which only the locus ucdcg-112 (0.244) and otgfa0_0007_B07 (0.263) were above 0.2. The average polymorphic information content (*PIC*) for all loci was 0.749, including 13 highly polymorphic loci ($PIC > 0.5$) and 2 moderately polymorphic loci ($0.25 < PIC < 0.5$) (Botstein et al., 1980). The overall high polymorphism allowed the 15 loci to accurately assess genetic diversity and genetic differentiation among populations.

Genetic diversity indices of each shell color and wild population are summarized in Table 3. The average number of alleles (N_a) for the 15 microsatellite loci ranged from 4.07 to 7.67 in shell color strains and from 11.73 to 13.60 in wild populations, while the effective number of alleles (N_e) ranged from 3.39 to 5.70 and from 6.50 to 7.58, respectively. We observed little difference in microsatellite diversity among all wild populations, but the N_a and N_e values of the orange shell strain (SO) were significantly lower than those of the other three strains (Kruskal-Wallis test: $P < 0.05$). Compared with wild populations, a significant decline in N_a (37.8–67.5%) and N_e (17.3–50.8%) was observed in shell color strains ($P < 0.05$). However, the reduction of alleles was not followed by an immediate decrease in heterozygosity, since no significant differences in H_o and H_e were observed between the wild and shell color

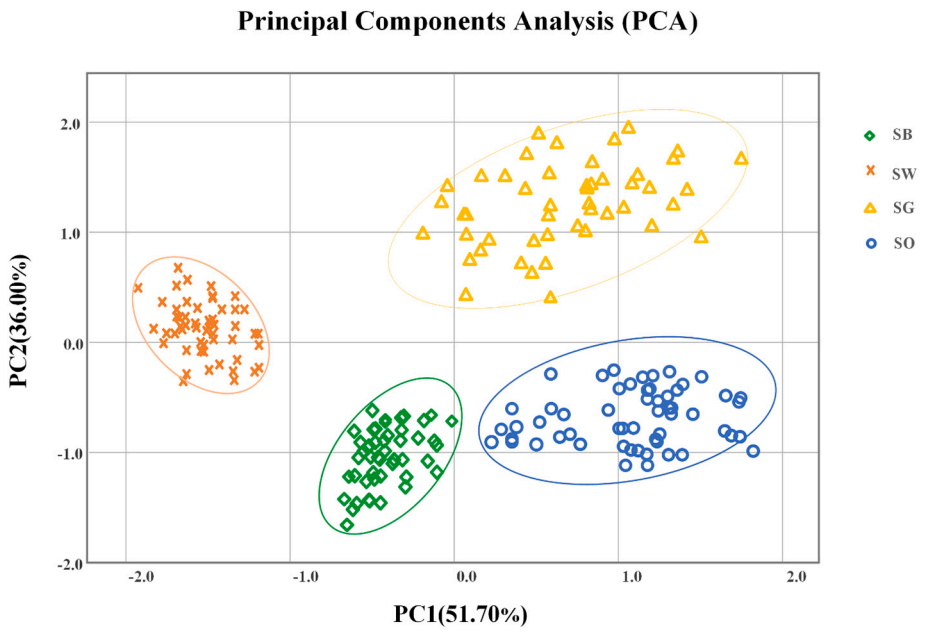

Fig. 2. Principal component analysis (PCA) of 192 individuals from four shell color strains based on color parameters.

Table 3
Genetic diversity parameters in shell color strains and wild populations of *C. gigas* based on 15 microsatellite loci.

Population	*N*	N_a	N_e	*I*	H_o	H_e	*PIC*	F_{is}^R/F_{is}^C	dHW^R/dHW^C
Shell color strains									
SB	96	6.40 ± 0.84^b	5.16 ± 0.47^b	1.36	0.66 ± 0.07^{ab}	0.69 ± 0.06^{ab}	0.54	0.11/−0.04	10/4
SW	115	7.67 ± 1.07^b	5.70 ± 0.55^b	1.55	0.63 ± 0.07^{ab}	0.75 ± 0.06^{ab}	0.60	0.17/0.08	9/3
SG	84	5.60 ± 0.60^b	4.63 ± 0.30^b	1.27	0.65 ± 0.06^{ab}	0.67 ± 0.04^{bc}	0.51	0.19/0.02	11/4
SO	61	4.07 ± 0.56^c	3.39 ± 0.32^c	0.98	0.52 ± 0.08^b	0.59 ± 0.07^c	0.44	0.29/0.12	12/5
Wild populations									
LYG	204	13.60 ± 1.56^a	7.58 ± 1.41^a	2.23	0.74 ± 0.03^a	0.85 ± 0.05^a	0.76	0.01/−0.17	2/0
QD	194	12.93 ± 1.70^a	6.70 ± 1.37^a	2.08	0.78 ± 0.03^a	0.82 ± 0.02^a	0.72	0.04/−0.11	2/1
RC	176	11.73 ± 1.53^a	6.50 ± 1.33^a	2.02	0.75 ± 0.04^a	0.82 ± 0.02^a	0.68	0.07/0.01	4/2
ZS	179	11.93 ± 1.52^a	6.80 ± 1.47^a	2.06	0.79 ± 0.05^a	0.83 ± 0.02^a	0.71	0.04/−0.21	2/0

N: number of alleles, N_a: average number of alleles, N_e: number of effective alleles, *I*: Shannon Wiener index, H_o: observed heterozygosity, H_e: expected heterozygosity, *PIC*: polymorphic information content, $^R F_{is}$: inbreeding coefficient calculated by raw data, $^C F_{is}$: inbreeding coefficient calculated by corrected data, dHW^R: number of loci deviating from Hardy-Weinberg equilibrium using raw data, dHW^C: number of loci deviating from Hardy-Weinberg equilibrium using corrected data. Means in the same column superscripted by different letters were significantly different ($P < 0.05$).

populations ($P < 0.05$). Besides, all H_o values were lower than those expected, suggesting that deficits of heterozygotes were prevalent in both wild and breeding populations. Similarly, the positive inbreeding coefficient values (F_{is}), between 0.01 (LYG) and 0.29 (SO), highlighted heterozygote deficiency again. In terms of comprehensive indicators, the Shannon-Wiener index (*I*) ranged from 0.98 to 2.23, and the *PIC* values from 0.44 to 0.76. With the exception of SO, the *I* and *PIC* values of other populations were all greater than 1.0 and 0.5, respectively, indicating high polymorphism (Botstein et al., 1980).

After the sequential Bonferroni correction, 52 out of the 120 locus-population combinations deviated from Hardy-Weinberg equilibrium (*HWE*), especially for locus ucdCg-198, ucdCg-117, otgfa0_0007_B07, and otgfa0_0139_G12 where all the populations showed significant deviation. After correcting the data for null alleles, the number of deviations from *HWE* was reduced from 42 to 16 in shell color strains and from 10 to 3 in wild populations (Table 3). Significant heterozygote deficiency could not be found, since the corrected F_{is} values changed from 0.01–0.29 to −0.21–0.12. In addition, the observed and expected heterozygosity after correction were higher than the raw data, and the values of H_o were no longer consistently lower than H_e (data not shown).

After sequence alignment, the 607-bp fragments of the mitochondrial COI gene generated from 80 oysters in shell color strains were obtained. Combined with the 18 mtCOI haplotypes identified in the four wild populations by Chen et al. (2022), a total of 23 haplotypes were used for further analysis, 17 of which were private, sharing 6 haplotypes (Table 4). The Median-joining (MJ) network is dominated by a major haplotype shared by all 8 populations (Fig. 3). Haplotype 1 (Hap_1) with a prevalence of 78.13% (125/160) across individuals was at the center, with other low-frequency haplotypes scattered around. The number of haplotypes (N_h) ranged from 3 to 11 in wild populations and from 1 to 5 in shell color strains. Except for the SO with one shared haplotype only, the other populations have their own unique haplotypes. Overall, the average haplotype diversity (H_d) and percent nucleotide diversity (P_i) of wild populations were higher than those of shell color strains. Similar to microsatellite data, the minimum values of mtDNA diversity index were all found in the SO.

3.3. Effective population size

Estimates of current effective population sizes (N_b) based on linkage disequilibrium showed a large difference between wild and shell color populations (Table 1). The N_b ranged from 198.3 (QD) to 595.3 (LYG) in

Table 4
Genetic diversity and haplotype frequency of mtCOI sequences observed among shell color strains and wild populations of *C. gigas*.

Haplotype	Shell color strains				Wild populations				Total
	SB	SW	SG	SO	LYG	QD	RC	ZS	160
	20	20	20	20	20	20	20	20	
Hap_1	12	19	19	20	12	10	16	17	125
Hap_2					3			1	4
Hap_3								1	1
Hap_4							1		1
Hap_5							1		1
Hap_6							1		1
Hap_7							1		1
Hap_8						1			1
Hap_9			1			1			2
Hap_10						1			1
Hap_11					1	1			2
Hap_12						1			1
Hap_13						1			1
Hap_14						1			1
Hap_15					2	1			3
Hap_16						1			1
Hap_17					1	1			2
Hap_18					1				1
Hap_19		1							1
Hap_20	5								5
Hap_21	1								1
Hap_22	1								1
Hap_23	1								1
N_h	5	2	2	1	6	11	5	3	
H_d	0.600 ± 0.101	0.100 ± 0.088	0.100 ± 0.088	0.000	0.632 ± 0.113	0.763 ± 0.103	0.368 ± 0.135	0.205 ± 0.119	
P_i (%)	0.152 ± 0.108	0.050 ± 0.081	0.017 ± 0.047	0.000	0.160 ± 0.048	0.368 ± 0.187	0.083 ± 0.036	0.053 ± 0.034	
k	0.921	0.300	0.100	0.000	0.958	2.200	0.500	0.316	

Haplotype: number of individuals for each haplotype, N_h: number of haplotypes, H_d: haplotype diversity (±standard deviations), P_i: percent nucleotide diversity (±standard deviations), k: average number of nucleotide differences.

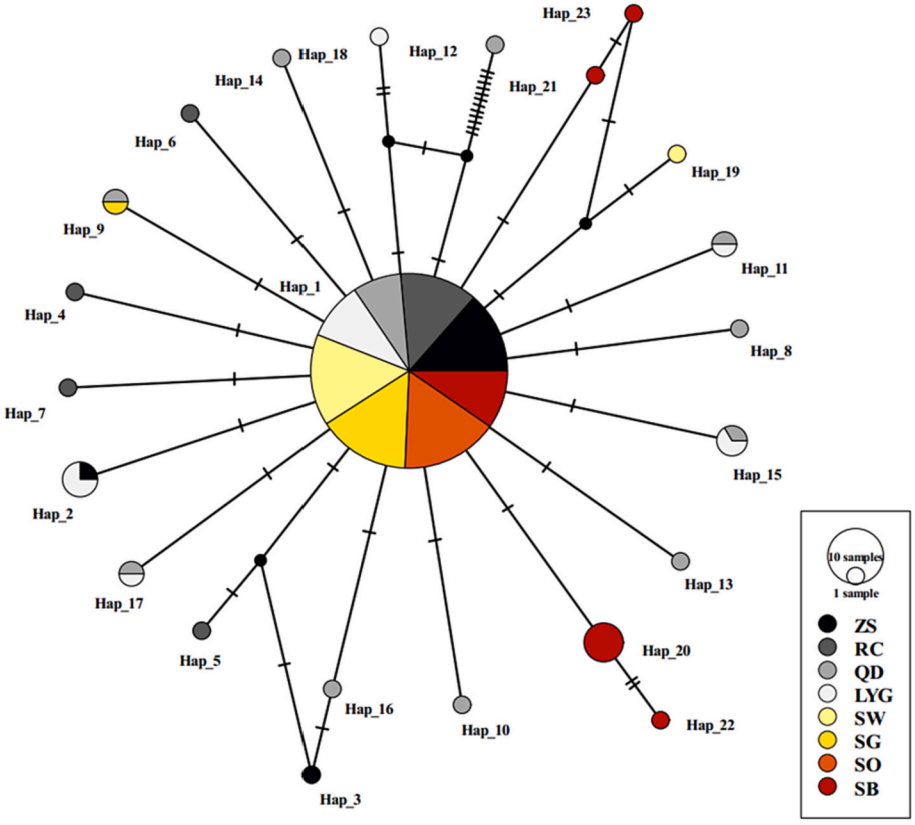

Fig. 3. Median-joining (MJ) networks for 23 COI haplotypes of shell color strains and wild populations of *C. gags*. The number of substitutions separating two haplotypes was indicated by the vertical bars on the line.

four wild populations, and from 66.4 (SO) to 86.7 (SB) in shell color strains. In addition, the N_b estimates exhibited a 13.3 to 33.6% decrease compared to the actual number of breeders used in each strain.

3.4. Genetic differentiation and clustering analysis

Analysis of molecular variances (AMOVA) revealed no significant genetic differentiation at all levels (among populations, among individuals within populations, and within individuals) for mitochondrial COI datasets ($P < 0.01$). Similarly, the Median-joining (MJ) network based on 23 COI haplotypes presented a typical 'star-like' topology dominated by one major haplotype, with no obvious genetic structure among populations (Fig. 3). For the nuclear microsatellite datasets, significant genetic differentiation was detected among shell color strains ($P < 0.01$), while only 2.69% of molecular genetic variances were found between different wild populations (Table 5). Besides, the predominant source of molecular variation was within individuals, both in shell color and wild populations.

Pairwise genetic differentiation coefficient (F_{ST}) calculated by microsatellites and mtCOI region are given in Table 6. Consistent with the result of mitochondrial AMOVA analysis, the pairwise F_{ST} values were generally low, with only a few populations genetically different from each other ($P < 0.05$). For microsatellites, the values of pairwise F_{ST} with a range of 0.267 to 0.121 characterized the high levels of genetic differentiation among four shell color strains, which is also supported by D_C with a range of 0.249 to 0.538 (data not shown). Besides, the maximal genetic identity of SB and SW ($F_{ST} = 0.121$; $D_C = 0.249$) and the strongest genetic difference between SG and SO ($F_{ST} = 0.267$; $D_C = 0.538$) were identified. In contrast, pairwise F_{ST} and D_C of wild samples were from 0.012 to 0.034 and from 0.145 to 0.309, respectively, only producing a weak trend of genetic divergence. Samples from ZS exhibited relatively high differences from other wild sampling sites included in the study. The assessment of the genetic differentiation between shell color strains and wild populations revealed moderate to high F_{ST} values ranging from 0.074 to 0.176 and D_C from 0.195 to 0.434. The principal coordinates analysis (PCoA) based on genetic distance matrices was conducted to further reveal the genetic relationships among populations and individuals (Fig. 5). Compared to wild populations, the boundaries of different shell color strains were easier to distinguish, while neither Coordinate axis 1 (7.29%) nor Coordinate axis 2 (7.01%) could completely separate the strains of the SB and SW, which confirmed a relatively high genetic similarity of the two strains.

When the clustering analysis was carried out on 192 oysters from shell color strains, the samples studied can be optimally divided into four theoretical groups, since the parameter curve of ΔK exhibited an extremely significant peak when K = 4. The genetic composition of each cluster was clearly divided, with a very low degree of genetic admixture at the individual level (Fig. 4a). When all 384 samples were included in the analysis, ΔK reached the highest value at K = 7. The genetic background of each shell color strain was completely separated and greatly differentiated from that of wild-collected oysters (Fig. 4b). In contrast, a high level of admixture was exhibited across all wild sampling locations, with samples from LYG and RC sharing similar genetic signatures and being grouped into one cluster.

Table 5
Analysis of molecular variances (AMOVA) for shell color strains and wild populations based on 15 microsatellite loci.

Source of variance	d.f.	Sum of squares	Variance components	Percentage of variation	F-statistics*
Among shell color strains					
Among populations	3	312.776	1.03828Va	19.43	F_{CT} = 0.19426*
Among individuals within populations	188	816.833	0.27779Vb	5.20	F_{SC} = 0.06451*
Within individuals	192	773.500	4.02865Vc	75.38	F_{ST} = 0.24624*
Total	383	1948.109	5.34471		
Among wild populations					
Among populations	3	67.073	0.15927Va	2.69	F_{CT} = 0.02695
Among individuals within populations	188	1328.729	1.31641Vb	22.27	F_{SC} = 0.22889*
Within individuals	192	851.500	4.43490Vc	75.03	F_{ST} = 0.24967*
Total	383	2247.302	5.91057		

* Significant at $P < 0.01$.

4. Discussion

Since the introduction of artificial selection in aquaculture, enormous numbers of aquatic animals have been purposefully bred for desirable economic traits, which has dramatically altered the genetic background of cultured breeds and ultimately changed the development prospects of the whole aquaculture industry (Gjedrem, 2012). In nature, the shell color of marine mollusks varies widely not only from species to species but also between different populations within the same species, providing substantial numbers of variants for selective breeding. Usually, shell pigmentation in bivalves is considered as a continuously distributed, quantitative trait with a gradual and sustained response to selection (Batista et al., 2008). For better shell color performance of the Pacific oyster, our selective breeding program has been consecutively conducted for 11–12 generations since 2010. Due to the great shape variation and bumpiness in oyster shells, traditional methods of measuring color properties, such as observing with naked eyes or using a colorimeter, are unreliable for assessing the effect of genetic improvement on shell color. Here, we made use of the computer vision system (CVS) to quantify shell color characteristics into colorimetric parameters of CIELAB, which eliminated the effects of surface roughness and contrived error, thereby enabling a non-destructive and objective evaluation. In this study, the chromatic values of L^*, a^*, and b^* varied significantly ($P < 0.05$) between different shell color strains, and individuals from each strain were closely gathered and completely separated from other strains in principal component analysis (PCA), evidencing the expected selection effect of shell color trait. The tightly clustered data points in PCA scatter plot implied a highly uniform color in the SB and SW strains, while relatively dispersive points indicated that the SO and SG strains have to be purified further. Previous studies identified differences in the heritability of shell pigments, which may account for the inconsistent progress in genetic improvement of different shell color strains (Brake et al., 2004).

For such polygenic, quantitative traits, which are strongly influenced by additive genetic variation, the achievement of genetic gains requires breeding strategies that accumulate favorable genes in the breeds over time using selection (Evans et al., 2009). Along with the continuous improvement of shell color traits, the identification and discrimination of four strains based on morphological criteria become increasingly clear. To further explore the genetic composition among these shell color-defined strains, the analysis of population simulation was conducted using microsatellite data, and four genetically differentiated clusters were identified based on the optimal number of subgroups. As expected, the boundaries of the inferred genetic clusters turned out to be completely concordant with the classification results based on distinct phenotypes of shell color, demonstrating that the populations with well-defined shell color have generated distinctive multi-locus combinations that render them genetically unique. Moreover, the pairwise F_{ST} calculated by microsatellites ranging from 0.267 to 0.121 and D_C from 0.249 to 0.538 further identify the high genetic heterogeneity among shell color strains. We, consequently, inferred that though the base

Table 6
Estimated pairwise F_{ST} values of *C. gigas* based on microsatellite makers (above diagonal) and mtDNA COI (below diagonal).

	SB	SW	SG	SO	LYG	QD	RC	ZS
SB	–	0.121*	0.206*	0.220*	0.094*	0.120*	0.126*	0.131*
SW	0.088*	–	0.181*	0.166*	0.074*	0.095*	0.101*	0.090*
SG	0.063*	0.016	–	0.267*	0.147*	0.153*	0.154*	0.158*
SO	0.049	0.011	0.101*	–	0.160*	0.176*	0.167*	0.152*
LYG	0.102	0.020	0.041	0.038	–	0.027	0.025	0.030*
QD	0.049	0.006	0.037	0.010	0.003	–	0.012	0.033*
RC	0.112*	0.001	0.002	0.006	−0.008	−0.003	–	0.034*
ZS	0.003	0.007	0.093*	0.003	0.005	0.013	0.009	–

The significance of population pairwise F_{ST} tested by 1000 permutations.
* Significantly at $P < 0.05$.

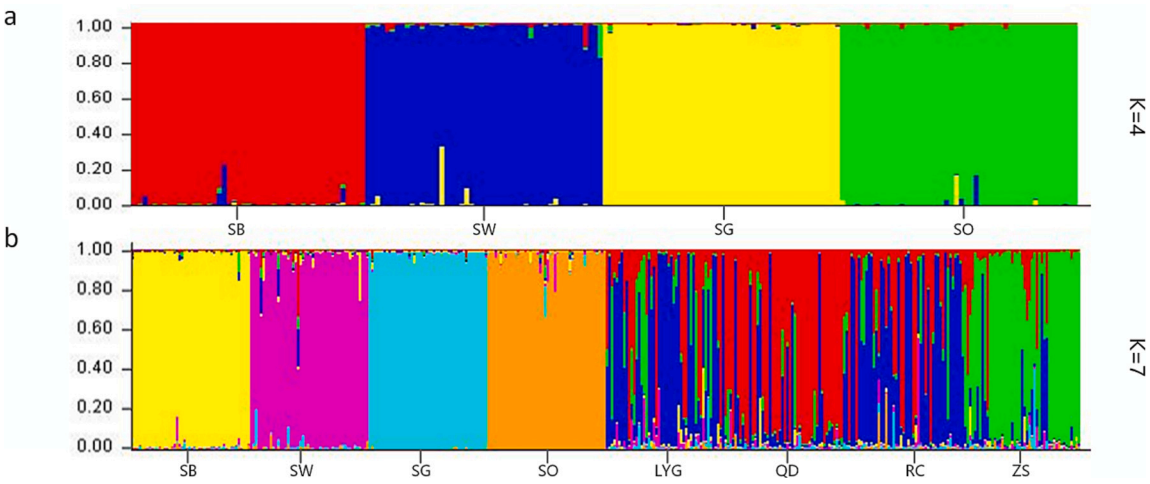

Fig. 4. Clustering analysis from STRUCTURE by 15 microsatellite datasets. Each vertical line represents an individual oyster, and each color represents a unique cluster detected by STRUCTURE. a. Proportion of the genome of each individual from shell color strains assigned to the four clusters (K = 4). b. Proportion of the genome of each individual from shell color strains and wild populations assigned to the seven clusters (K = 7).

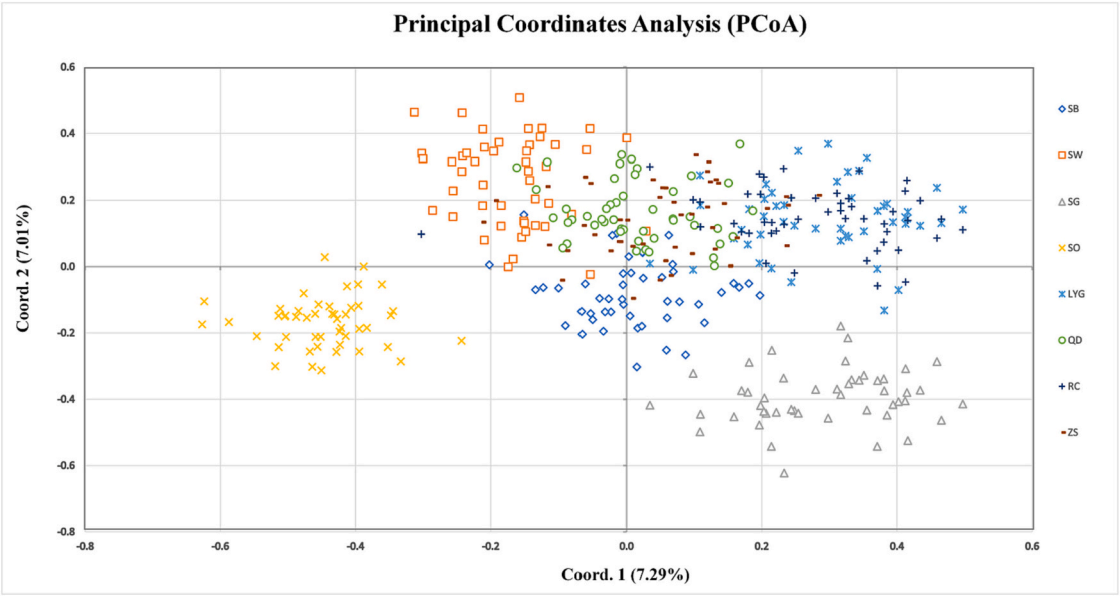

Fig. 5. Principal coordinates analysis (PCoA) of 384 individuals from eight populations based on genetic distance matrices. The different populations are indicated by different colors and symbols, respectively.

population of each color strain was a subset of the original stock located in Shandong, the four varieties may have become less representative of the initial ancestries after deep division. When wild oysters distributed in different sampling areas were added, all oysters can be optimally assigned to seven genetically similar groups. The clustering analysis clearly differentiated each shell color strain from wild oysters, while differences within wild populations were comparatively less pronounced. However, the 'star-like' haplotype network generated from

mitochondrial COI data showed that no obvious mtDNA branches or genetic clusters were formed in all samples. This is because microsatellite markers, by contrast, possess a faster rate of mutation and are therefore more susceptible to selection and drift, both of which are more likely to take place during artificial breeding (Bruford and Wayne, 1993).

For conspecific populations, the level of genetic structuring depends largely on the evolutionary forces that either homogenize genetic resources or promote divergence (Bruford et al., 2003). Strong positive selection was a vital driver in shaping heterogeneous structures among shell color strains (Zou et al., 2014), and strict breeding measures to separate and preserve phenotypically distinct sets, ultimately creating the barrier to gene flow, also played an important role. Additionally, samples of shell color strains were highly differentiated from those of wild populations, which was either due to inherent genetic differences from the original population or a genetic drift phenomenon caused by a few founders (Hillen et al., 2017). However, our observation of weak genetic differentiation (F_{ST}: 0.012–0.034; D_C: 0.145–0.309) among wild *C. gigas* populations is not unexpected. Many marine organisms including most bivalves were less geographically differentiated, as a result of widespread dispersal capability and intricate hydrology conditions (Naaykens and D'Aloia, 2022; Thomas and Miller, 2022; Yu and Chu, 2006). The considerable genetically admixed individuals in the STRUCTURE plots also suggested the strong genetic connectivity across all geographical groupings. Consistently, the genetic boundary of wild populations was not distinct with high overlapping by PCoA analysis, while individuals from each shell color strain tended to cluster together and stood out from other strains, indicating high genetic uniformity within strains and great genetic divergence among strains.

In aquaculture, genetic diversity is closely related not only to biological survivability but also to the response to selection, however, it might be gradually eroded in the face of continuous selection pressures (Varney and Wilbur, 2020). Thus, it is essential to monitor the trend in genetic diversity, which will inform further management and conservation to ensure the achievement of desired gains. The use of nuclear microsatellites and mtCOI sequences here is expected to elucidate whether the present shell color strains contain adequate genetic diversity on which further genetic gains and improvements rely. It is well accepted that the Shannon-Wiener index (*I*) and the polymorphism information content (*PIC*), which can reflect the richness and heterozygosity of alleles in an integrated manner, are two of the most important indicators of genetic diversity. In this study, the *PIC* value ranged from 0.44 (SO) to 0.60 (SW) with an average of 0.52, and the Shannon-Wiener index (*I*) changed from 0.98 (SO) to 1.55 (SW) with a mean value of 1.29, supporting overall high polymorphism and rich allelic contents possessed by shell color strains (Botstein et al., 1980). The higher genetic diversity compared with other cultured stocks of aquatic species benefitted from our breeding practices such as balancing sex ratio, expanding population size, controlling inbreeding level, as well as the selection intensity tailored to each color strain (Han et al., 2019; Xing et al., 2017). In addition, we combined growth performance as our joint breeding target in generations of mass selection (Xu et al., 2019), which can effectively avoid selecting individuals just from a few families with the best performance of coloration character, thereby conducing to maintaining a relatively rich gene bank during the long-term breeding program.

Despite the sufficient genetic information contained in the shell color strains, a tendency of reduced alleles, with an overall 52.65% drop in *Na* and 34.05% drop in *Ne*, was identified compared to outbred wild populations. The number of mtCOI haplotypes also exhibited a similar decline. This may be a corollary of selection effects that occurred during (i) the choice of original parents–generally, segregating broodstocks from the wild result in a sharp shrinkage of genetic information content; and (ii) three to four generations of family selection aimed at eliminating variegated phenotypes, frequently followed by the loss of rare alleles and minor haplotypes. By contrast, heterozygosity is much less sensitive to genetic change than the number of alleles, consistently with the prior result obtained in other selected strains of aquatic species (Appleyard and Ward, 2006; Hillen et al., 2017). Remarkably, the orange-shell variant suffered the greatest loss of diversity and scored the lowest values for all genetic diversity indices both in mtCOI and microsatellite datasets (Tables 3 and 4). According to the reports by Cong et al. (2014) and Han et al. (2019), the SB, SG, and SW strains were initially selected from large-scale wild populations containing wealthy genetic information, whereas the first generation of SO was constructed by only four variants accidentally detected in the hybrid offspring of cultivated oysters. Thus, it is the limited founders that restricted the genetic diversity of the SO strain, which suggests capturing large numbers of genotypes at the beginning was extremely important for the long-term sustainability of breeding lines of oysters. If a small number of parents cannot be avoided, like rare orange shell oysters in this case, the deficiency of initial genotypes can be partly compensated by cross-breeding of strains rich in variation (Evans et al., 2004b). That is, of course, provided that such hybridization won't cause the degeneration of well-defined traits.

The occurrence of heterozygote deficits related to Hardy-Weinberg disequilibrium is a common population-genetic phenomenon in microsatellite surveys of marine mollusks (De Meeus, 2018; Lemer and Planes, 2012). The populations under study, whether they were cultured or wild, exhibited significant deficits of heterozygotes, as shown by the disparity between expected and observed heterozygosity as well as the fact that all of the F_{is} values were positive. Previously, a strong correlation between heterozygote deficits and null alleles was documented in plenty of marine or freshwater bivalves (Astanei et al., 2005; Yu et al., 2015). Similarly, correcting the data set for null alleles made heterozygote deficiency less pronounced and decreased the number of loci deviating from *HWE* from 52 to 19 in this study. Additionally, both using raw and corrected data, deficits of heterozygotes in shell color strains were more prevalent than in the wild as a result of typical small population processes such as founder effects, inbreeding, and non-random mating (Chen et al., 2017; Hansen et al., 2001).

When analyzing the effective population size (N_b) of shell color strains separately, results showed that the SB had a larger effective population size than the other three strains, but even so, the N_b was 13.3% lower than the actual number of spawning individuals. This does not seem surprising, as this phenomenon is prevalent in oysters and other marine organisms that have in common a tendency for unbalanced parental contributions, i.e., sweepstakes reproductive success (Saura et al., 2021). Simultaneously, due to the limitations of small broodstock size, different viability of gametes, etc., the effective population size would inevitably decay over time during the artificial breeding process (Brown et al., 2005). The N_b estimates, as expected, ranged from 66.4 (SO) to 86.7 (SB) in the four shell color strains, which were significantly lower than that of the wild populations ranging from 198.3 (QD) to 595.3 (LYG). This general result was also observed by Lallias et al. (2010) in the flat oyster and by Hu et al. (2022) in the Iwagaki oyster, using microsatellite markers. At present, a consensus rule emerging from animal breeding programs is that the minimum effective population size to avoid severe inbreeding depression and to survive in the short-term is around 50, which corresponds to a 1% increase in inbreeding per generation (Villanueva et al., 2022). Encouragingly, the breeding measures we have taken may have contributed to the N_b estimates above the critical size of 50 for all shell color strains, for example, artificial spawning during the breeding process could better control the contribution of gamete and somewhat narrowed the reproductive or survival differences between parents. In addition, most wild populations of *C. gigas* in this study showed N_b estimates higher than 400, with only the QD being less than 200. It is likely that the significantly lower N_b estimate in QD is due to large-scale breeding programs in surrounding areas diluting the natural gene pool of *C. gigas*, resulting in fewer families represented in the samples.

In conclusion, the four selected strains of *C. gigas* with distinct shell

color characteristics are sufficiently genetically diverse and highly differentiated from wild populations. Although the process of artificial selection had some effects on the genetic diversity and genetic structure, the four shell color strains still have the potential to continually increase genetic gains in future generations. It is indicated that the problem of inbreeding depression or genetic homogenization in shell color strains has not been ignored, and current breeding approaches help to achieve a balance between phenotypic improvement and genetic health. The present investigation provides important information for future genetic improvement and management of these valuable resources.

CRediT authorship contribution statement

Yifei Zhang: Conceptualization, Investigation, Methodology, Data curation, Writing – original draft. **Yulu Chen:** Methodology, Data curation. **Chengxun Xu:** Supervision, Writing – review & editing. **Qi Li:** Writing – review & editing.

Declaration of Competing Interest

The authors declare that they have no known competing financial interests or personal relationships that could have appeared to influence the work reported in this paper.

Data availability

Data will be made available on request.

Acknowledgments

This work was supported by the China Agriculture Research System Project (CARS-49), and Earmarked Fund for Agriculture Seed Improvement Project of Shandong Province (2020LZGC016, 2021LZGC027).

References

Appleyard, S.A., Ward, R.D., 2006. Genetic diversity and effective population size in mass selection lines of Pacific oyster (*Crassostrea gigas*). Aquaculture. 254, 148–159.
Astanei, I., Gosling, E., Wilson, J., Powell, E., 2005. Genetic variability and phylogeography of the invasive zebra mussel, *Dreissena polymorpha* (Pallas). Mol. Ecol. 14, 1655–1666.
Bandelt, H.J., Forster, P., Röhl, A., 1999. Median-joining networks for inferring intraspecific phylogenies. Mol. Biol. Evol. 16, 37–48.
Batista, F.M., Ben-Hamadou, R., Fonseca, V.G., Taris, N., Ruano, F., Reis-Henriques, M. A., Boudry, P., 2008. Comparative study of shell shape and muscle scar pigmentation in the closely related cupped oysters, *Crassostrea angulata*, *C. gigas* and their reciprocal hybrids. Aquat. Living Resour. 21, 31–38.
Berrebi, P., Horvath, Á., Splendiani, A., Palm, S., Bernaś, R., 2021. Genetic diversity of domestic brown trout stocks in Europe. Aquaculture. 544, 737043.
Botstein, D., White, R.L., Skolnick, M., Davis, R.W., 1980. Construction of a genetic linkage map in man using restriction fragment length polymorphisms. Am. J. Hum. Genet. 32, 314–331.
Boudry, P., Collet, B., Cornette, F., Hervouet, V., Bonhomme, F., 2002. High variance in reproductive success of the Pacific oyster (*Crassostrea gigas*, Thunberg) revealed by microsatellite-based parentage analysis of multifactorial crosses. Aquaculture. 204, 283–296.
Brake, J., Evans, F., Langdon, C., 2004. Evidence for genetic control of pigmentation of shell and mantle edge in selected families of Pacific oysters, *Crassostrea gigas*. Aquaculture. 229, 89–98.
Brown, C., Woolliams, J.A., McAndrew, B.J., 2005. Factors influencing effective population size in commercial populations of gilthead seabream, *Sparus aurata*. Aquaculture. 247, 219–225.
Bruford, M.W., Wayne, R.K., 1993. Microsatellites and their application to population genetics. Curr. Opin. Genet. Dev. 3, 939–943.
Bruford, M.W., Bradley, D.G., Luikart, G., 2003. DNA markers reveal the complexity of livestock domestication. Nat. Rev. Genet. 4, 900–910.
Budd, A., McDougall, C., Green, K., Degnan, B.M., 2014. Control of shell pigmentation by secretory tubules in the abalone mantle. Front. Zool. 11, 1–9.
Chapuis, M.P., Estoup, A., 2007. Microsatellite null alleles and estimation of population differentiation. Mol. Biol. Evol. 24, 621–631.
Chapuis, M.P., Lecoq, M., Michalakis, Y., Loiseau, A., Sword, G.A., Piry, S., Estoup, A., 2008. Do outbreaks affect genetic population structure? A worldwide survey in Locusta migratoria, a pest plagued by microsatellite null alleles. Mol. Ecol. 17, 3640–3653.
Chen, N., Luo, X., Lu, C., Ke, C., You, W., 2017. Effects of artificial selection practices on loss of genetic diversity in the Pacific abalone, *Haliotis discus hannai*. Aquac. Res. 48, 4923–4933.
Chen, Y., Xu, C., Li, Q., 2022. Genetic diversity in a genetically improved line of the Pacific oyster *Crassostrea gigas* with orange shell based on microsatellites and mtDNA data. Aquaculture. 549, 737791.
Cong, R., Li, Q., Ge, J., Kong, L., Yu, H., 2014. Comparison of phenotypic traits of four shell color families of the Pacific oyster (*Crassostrea gigas*). J. Fish. Sci. Chin. 21, 494–502.
De Meeus, T., 2018. Revisiting F-IS, F-ST, Wahlund effects, and null alleles. J. Hered. 109, 446–456.
Dégremont, L., Bédier, E., Boudry, P., 2010. Summer mortality of hatchery-produced Pacific oyster spat (*Crassostrea gigas*). II. Response to selection for survival and its influence on growth and yield. Aquaculture. 299, 21–29.
Do, C., Waples, R.S., Peel, D., Macbeth, G., Tillett, B.J., Ovenden, J.R., 2014. NeEstimator v2: re-implementation of software for the estimation of contemporary effective population size (N_e) from genetic data. Mol. Ecol. Resour. 14, 209–214.
Evanno, G., Regnaut, S., Goudet, J., 2005. Detecting the number of clusters of individuals using the software STRUCTURE: a simulation study. Mol. Ecol. 14, 2611–2620.
Evans, B., Bartlett, J., Sweijd, N., Cook, P., Elliott, N.G., 2004a. Loss of genetic variation at microsatellite loci in hatchery produced abalone in Australia (*Haliotis rubra*) and South Africa (*Haliotis midae*). Aquaculture. 233, 109–127.
Evans, F., Matson, S., Brake, J., Langdon, C., 2004b. The effects of inbreeding on performance traits of adult Pacific oysters (*Crassostrea gigas*). Aquaculture. 230, 89–98.
Evans, S., Camara, M.D., Langdon, C.J., 2009. Heritability of shell pigmentation in the Pacific oyster, *Crassostrea gigas*. Aquaculture. 286, 211–216.
Excoffier, L., Lischer, H.E., 2010. Arlequin suite ver 3.5: a new series of programs to perform population genetics analyses under Linux and windows. Mol. Ecol. Resour. 10, 564–567.
Falush, D., Stephens, M., Pritchard, J.K., 2003. Inference of population structure using multilocus genotype data: linked loci and correlated allele frequencies. Genetics. 164, 1567–1587.
Gjedrem, T., 2012. Genetic improvement for the development of efficient global aquaculture: a personal opinion review. Aquaculture. 344, 12–22.
Han, Z., Li, Q., Liu, S., Yu, H., Kong, L., 2019. Genetic variability of an orange-shell line of the Pacific oyster *Crassostrea gigas* during artificial selection inferred from microsatellites and mitochondrial COI sequences. Aquaculture. 508, 159–166.
Hansen, M.M., Ruzzante, D.E., Nielsen, E.E., Mensberg, K.L.D., 2001. Brown trout (*Salmo trutta*) stocking impact assessment using microsatellite DNA markers. Ecol. Appl. 11, 148–160.
Hillen, J., Coscia, I., Vandeputte, M., Herten, K., Hellemans, B., Maroso, F., Vergnet, A., Allal, F., Maes, G., Volckaert, F., 2017. Estimates of genetic variability and inbreeding in experimentally selected populations of European sea bass. Aquaculture. 479, 742–749.
Hu, Y., Li, Q., Xu, C., Liu, S., Kong, L., Yu, H., 2022. Genetic variability of mass-selected and wild populations of Iwagaki oyster (*Crassostrea nippona*) revealed by microsatellites and mitochondrial COI sequences. Aquaculture. 561.
Kahn, B.E., Wansink, B., 2004. The influence of assortment structure on perceived variety and consumption quantities. J. Con. Res. 30, 519–533.
Kalinowski, S.T., Taper, M.L., Marshall, T.C., 2007. Revising how the computer program CERVUS accommodates genotyping error increases success in paternity assignment. Mol. Ecol. 16, 1099–1106.
Kang, J.-H., Kang, H.-S., Lee, J.-M., An, C.-M., Kim, S.-Y., Lee, Y.-M., Kim, J.-J., 2013. Characterizations of shell and mantle edge pigmentation of a Pacific oyster, *Crassostrea gigas*, in Korean peninsula. Asian-Australas J. Anim. Sci. 26, 1659.
Lallias, D., Boudry, P., Lapegue, S., King, J.W., Beaumont, A.R., 2010. Strategies for the retention of high genetic variability in European flat oyster (*Ostrea edulis*) restoration programmes. Conserv. Genet. 11, 1899–1910.
Leigh, J.W., Bryant, D., 2015. Popart: full-feature software for haplotype network construction. Methods Ecol. Evol. 6, 1110–1116.
Lemer, S., Planes, S., 2012. Translocation of wild populations: conservation implications for the genetic diversity of the black-lipped pearl oyster *Pinctada margaritifera*. Mol. Ecol. 21, 2949–2962.
Li, G., Hubert, S., Bucklin, K., Ribes, V., Hedgecock, D., 2003. Characterization of 79 microsatellite DNA markers in the Pacific oyster *Crassostrea gigas*. Mol. Ecol. Resour. 3, 228–232.
Li, Q., Yu, H., Yu, R., 2006. Genetic variability assessed by microsatellites in cultured populations of the Pacific oyster (*Crassostrea gigas*) in China. Aquaculture. 259, 95–102.
Li, Q., Wang, Q., Liu, S., Kong, L., 2011. Selection response and realized heritability for growth in three stocks of the Pacific oyster *Crassostrea gigas*. Fish. Sci. 77, 643–648.
Librado, P., Rozas, J., 2009. DnaSP v5: a software for comprehensive analysis of DNA polymorphism data. Bioinformatics. 25, 1451–1452.
Liu, T., Li, Q., Song, J., Yu, H., 2017. Development of genomic microsatellite multiplex PCR using dye-labeled universal primer and its validation in pedigree analysis of Pacific oyster (*Crassostrea gigas*). J. Ocean U. China 16, 151–160.
Marchais, V., Jolivet, A., Herve, S., Roussel, S., Schoene, B.R., Grall, J., Chauvaud, L., Clavier, J., 2017. New tool to elucidate the diet of the ormer *Haliotis tuberculata* (L.): Digital shell color analysis. Mar. Biol. 164, 1–13.
Naaykens, T., D'Aloia, C.C., 2022. Isolation-by-distance and genetic parentage analysis provide similar larval dispersal estimates. Mol. Ecol. 31, 3072–3082.
Nell, J.A., 2001. The history of oyster farming in Australia. Mar. Fish. Rev. 63, 14–25.
Nie, H.T., Jiang, K.Y., Jiang, L.W., Huo, Z.M., Ding, J.F., Yan, X.W., 2020. Transcriptome analysis reveals the pigmentation related genes in four different shell color strains of the Manila clam *Ruditapes philippinarum*. Genomics. 112, 2011–2020.

Peakall, R., Smouse, P.E., 2012. GenAlEx 6.5: genetic analysis in Excel. Population genetic software for teaching and research—an update. Bioinformatics. 28, 2537–2539.
Pedreschi, F., Leon, J., Mery, D., Moyano, P., 2006. Development of a computer vision system to measure the color of potato chips. Food Res. Int. 39, 1092–1098.
Phifer-Rixey, M., Heckman, M., Trussell, G.C., Schmidt, P.S., 2008. Maintenance of clinal variation for shell colour phenotype in the flat periwinkle *Littorina obtusata*. J. Evolution. Biol. 21, 966–978.
Qi, H., Wu, Q., Li, L., Zhang, G., 2009. Development and characterization of microsatellite markers for the Pacific oyster *Crassostrea gigas*. Conserv. Genet. Resour. 1, 451–453.
Rousset, R., 1995. Population genetics software for exact tests and ecumenicism. J. Hered. 86, 248–249.
Saura, M., Caballero, A., Santiago, E., Fernandez, A., Morales-Gonzalez, E., et al., 2021. Estimates of recent and historical effective population size in turbot, seabream, seabass and carp selective breeding programmes. Genet. Sel. Evol. 53, 85.
Sauvage, C., Boudry, P., Lapegue, S., 2009. Identification and characterization of 18 novel polymorphic microsatellite makers derived from expressed sequence tags in the Pacific oyster *Crassostrea gigas*. Mol. Ecol. Resour. 9, 853–855.
Sekino, M., Hamaguchi, M., Aranishi, F., Okoshi, K., 2003. Development of novel microsatellite DNA markers from the Pacific oyster *Crassostrea gigas*. Mar. Biotechnol. 5, 227–233.
Sokolova, I.M., Berger, V.J., 2000. Physiological variation related to shell colour polymorphism in White Sea *Littorina saxatilis*. J. Exp. Mar. Biol. Ecol. 245, 1–23.
Song, J., Li, Q., Zhong, X., Kong, L., Yu, H., 2017. Genetic diversity and outlier loci detecting of shell color variation in the Pacific oyster (*Crassostrea gigas*) by SNP markers. Aquat. Living Resour. 30, 10.
Tettelbach, S.T., Furman, B.T., Hughes, S.W.T., Carroll, J.M., Peterson, B.J., Havelin, J., Tettelbach, C.R.H., Patricio, R.M., 2020. Attempted use of an uncommon bay scallop color morph for tracking the contribution of restoration efforts to population recovery. Restor. Ecol. 28, 532–542.
Thomas, L., Miller, K.J., 2022. High gene flow in the silverlip pearl oyster *Pinctada maxima* between inshore and offshore sites near eighty Mile Beach in Western Australia. PeerJ. 10, 13323.
Timmermans, A., 1998. Computer vision system for on-line sorting of pot plants based on learning techniques. Acta Hortic. 421, 91–98.
Van Oosterhout, C., Hutchinson, W.F., Wills, D.P., Shipley, P., 2004. MICRO-CHECKER: software for identifying and correcting genotyping errors in microsatellite data. Mol. Ecol. Notes 4, 535–538.
Varney, R.L., Wilbur, A.E., 2020. Analysis of genetic variation and inbreeding among three lines of hatchery-reared *Crassostrea virginica* broodstock. Aquaculture. 527, 735452.
Villanueva, B., Fernández, A., Peiró-Pastor, R., Peñaloza, C., Houston, R.D., Sonesson, A. K., Tsigenopoulos, C.S., Bargelloni, L., Gamsız, K., Karahan, B., Gökçek, E.Ö., Fernández, J., Saura, M., 2022. Population structure and genetic variability in wild and farmed Mediterranean populations of gilthead seabream and European seabass inferred from a 60K combined species SNP array. Aquac. Rep. 24, 101145.
Vrijenhoek, R., 1994. DNA primers for amplification of mitochondrial cytochrome c oxidase subunit I from diverse metazoan invertebrates. Mol. Mar. Biol. Biotechnol. 3, 294–299.
Wada, K.T., 1990. Inheritance of white coloration of the prismatic layer of shells in the Japanese pearl oyster, *Pinctada fucata martensii*, and its importance in the pearl culture industry. Aquaculture. 85, 1–4.
Wan, S., Li, Q., Liu, T., Yu, H., Kong, L., 2017. Heritability estimates for shell color-related traits in the golden shell strain of Pacific oyster (*Crassostrea gigas*) using a molecular pedigree. Aquaculture. 476, 65–71.
Wen, H., Gu, R., Cao, Z., Zhou, X., Nie, Z., Ge, X., Xu, P., Hua, D., 2013. Variation of color and ray pattern in juvenile shells in hatchery-produced freshwater triangle pearl mussels, *Hyriopsis cumingii*, in China. J. World. Aquacult. Soc. 44, 154–160.
Williams, S.T., 2017. Molluscan shell colour. Biol. Rev. 92, 1039–1058.
Winkler, F.M., Estevez, B.F., Jollan, L.B., Garrido, J.P., 2001. Inheritance of the general shell color in the scallop *Argopecten purpuratus* (Bivalvia: Pectinidae). J. Hered. 92, 521–525.
Xing, D., Li, Q., Zhang, J., 2017. Analysis of genetic diversity in mass selection lines of white-shell Pacific oyster (*Crassostrea gigas*) using microsatellite fluorescent multiplex PCR technique. J. Fish. China 41, 1838–1846.
Xu, L., Li, Q., Yu, H., Kong, L., 2017. Estimates of heritability for growth and shell color traits and their genetic correlations in the black shell strain of Pacific oyster *Crassostrea gigas*. Mar Biotechnol (NY). 19, 421–429.
Xu, L., Li, Q., Xu, C., Yu, H., Kong, L., 2019. Genetic diversity and effective population size in successive mass selected generations of black shell strain Pacific oyster (*Crassostrea gigas*) based on microsatellites and mtDNA data. Aquaculture. 500, 338–346.
Yam, K.L., Papadakis, S.E., 2004. A simple digital imaging method for measuring and analyzing color of food surfaces. J. Food Eng. 61, 137–142.
Yamtich, J., Voigt, M.L., Li, G., Hedgecock, D., 2005. Eight microsatellite loci for the Pacific oyster *Crassostrea gigas*. Anim. Genet. 36, 524–526.
Yu, D.H., Chu, K.H., 2006. Low genetic differentiation among widely separated populations of the pearl oyster *Pinctada fucata* as revealed by AFLP. J. Exp. Mar. Biol. Ecol. 333, 140–146.
Yu, H., Gao, S., Chen, A., Kong, L., Li, Q., 2015. Genetic diversity and population structure of the ark shell *Scapharca broughtonii* along the coast of China based on microsatellites. Biochem. Syst. Ecol. 58, 235–241.
Zheng, H., Zhang, G., Liu, X., 2005. Comparison of growth and survival of larvae among different shell color stocksof bay scallop *Argopecten irradians irradians* (Lamarck 1819). Chin. J. Oceanol. Limnol. 23, 183–188.
Zheng, H., Zhang, T., Sun, Z., Liu, W., Liu, H., 2013. Inheritance of shell colours in the noble scallop *Chlamys nobilis* (Bivalve: *Pectinidae*). Aquac. Res. 44, 1229–1235.
Zou, K., Zhang, D., Guo, H., Zhu, C., Li, M., Jiang, S., 2014. A preliminary study for identification of candidate AFLP markers under artificial selection for shell color in pearl oyster *Pinctada fucata*. Gene. 542, 8–15.